JPSS

Joint Polar Satellite System

VIIRS retrievals of *Karenia brevis* harmful algal blooms in the West Florida Shelf using Neural Networks.

Sam Ahmed[1], Ahmed El-Habashi[1] and Vincent Lovko[2].

NOAA Collaborators Drs. Richard P. Stumpf[3] and Michelle C. Tomlinson[3]

[1]NOAA CREST Optical Remote Sensing Laboratory, the City College of the City University of NY, USA

[2]Mote Marine Laboratories, Sarasota FL 34236

[3]NOAA National Centers for Coastal Ocean Science, 1305 East-West Highway code N/SCI1 Silver Spring, MD 20910, USA

Outline

- Background of Harmful Algal blooms (HABs) in West Florida Shelf (WFS)
- Neural Networks (*NN*) algorithm architecture
- *Karenia Brevis* Harmful Algal bloom (*KB*-HABs) retrieval approach
- Comparison of in-situ measurements vs. retrieval algorithms
- Consecutive satellite images showing variations
- Field measurements
- Conclusion

Background of *KB* HABS in WFS

- ➢ Harmful algal blooms, occur when colonies of phytoplankton grow out of control while producing toxic or harmful effects on people, fish, shellfish, marine mammals and birds.

- ➢ In united states it has been estimated that $30-$70 million is lost annually as a result of HABs (Fisher et al.). Recent July 4th 2016 bloom had a major effect on economy and health.

MODIS & VIIRS satellite capability for *KB* HABs detections

- MODIS retrieval of *KB* uses fluorescence line height technique (nFLH) which requires 678nm chlorophyll fluorescence band

- 678 nm band not available on VIIRS providing impetus for development of NN technique, which uses as inputs 486, 551 and 671 nm available in VIIRS.

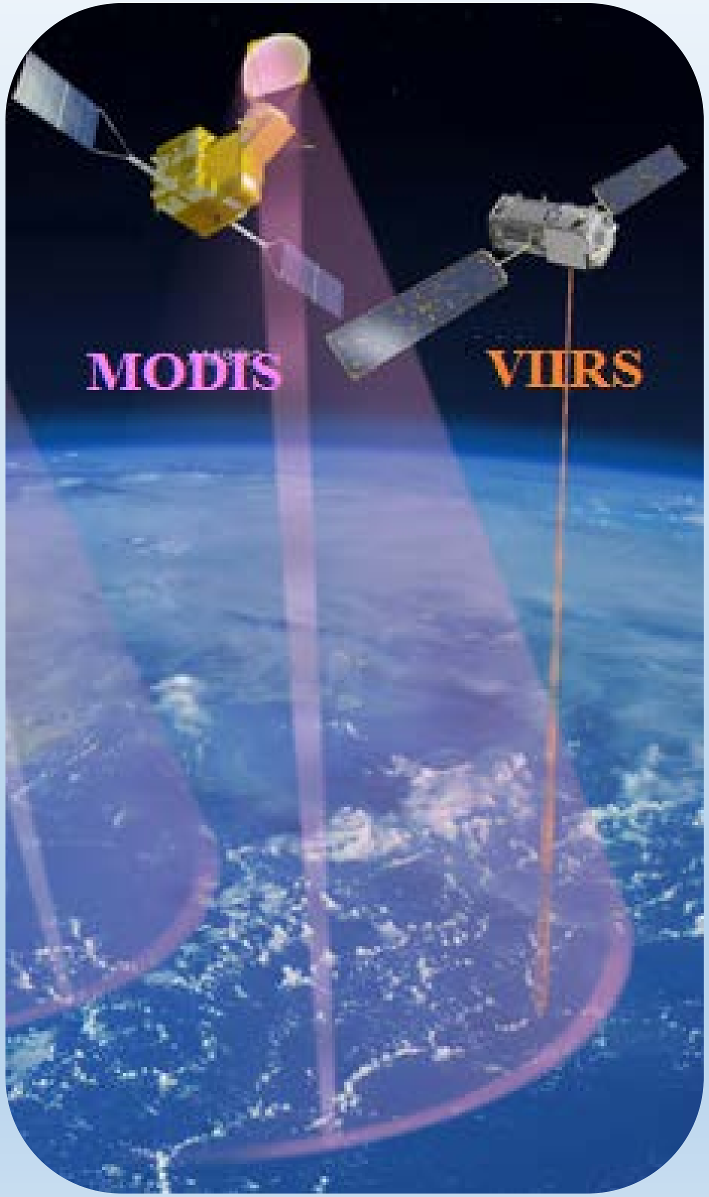

Neural Networks (NN) Algorithm Architecture.

- A multilayer perceptron neural network (NN) was developed based on a 4 component bio-optical (pure water, phytoplankton, CDOM and NAP): 20,000 simulated dataset generated as a random variables, based on a wide range of coastal and oceanic NOMAD IOPs, used in a forward bio-optical model based on radiative transfer, to generate 20,000 sets of Rrs at 486,551 and 671 nm (VIIRS bands)/

- NN was trained on 10,000 and tested and validated on remaining 10,000 simulated dataset and field measurements.

- Note: NN uses Rrs from VIIRS as inputs at 486, 551 & 671 nm, all relatively long wavelengths which are not greatly impacted by atmospheric correction inadequacies.

- Output of IOPs (aph etc) all at 443 which at the peak of aph and thus exhibit most variation (We are only interested at aph443)

Example of VIIRS *NN* retrievals of a_{ph443}, and its conversion to equivalent [*Chla*].

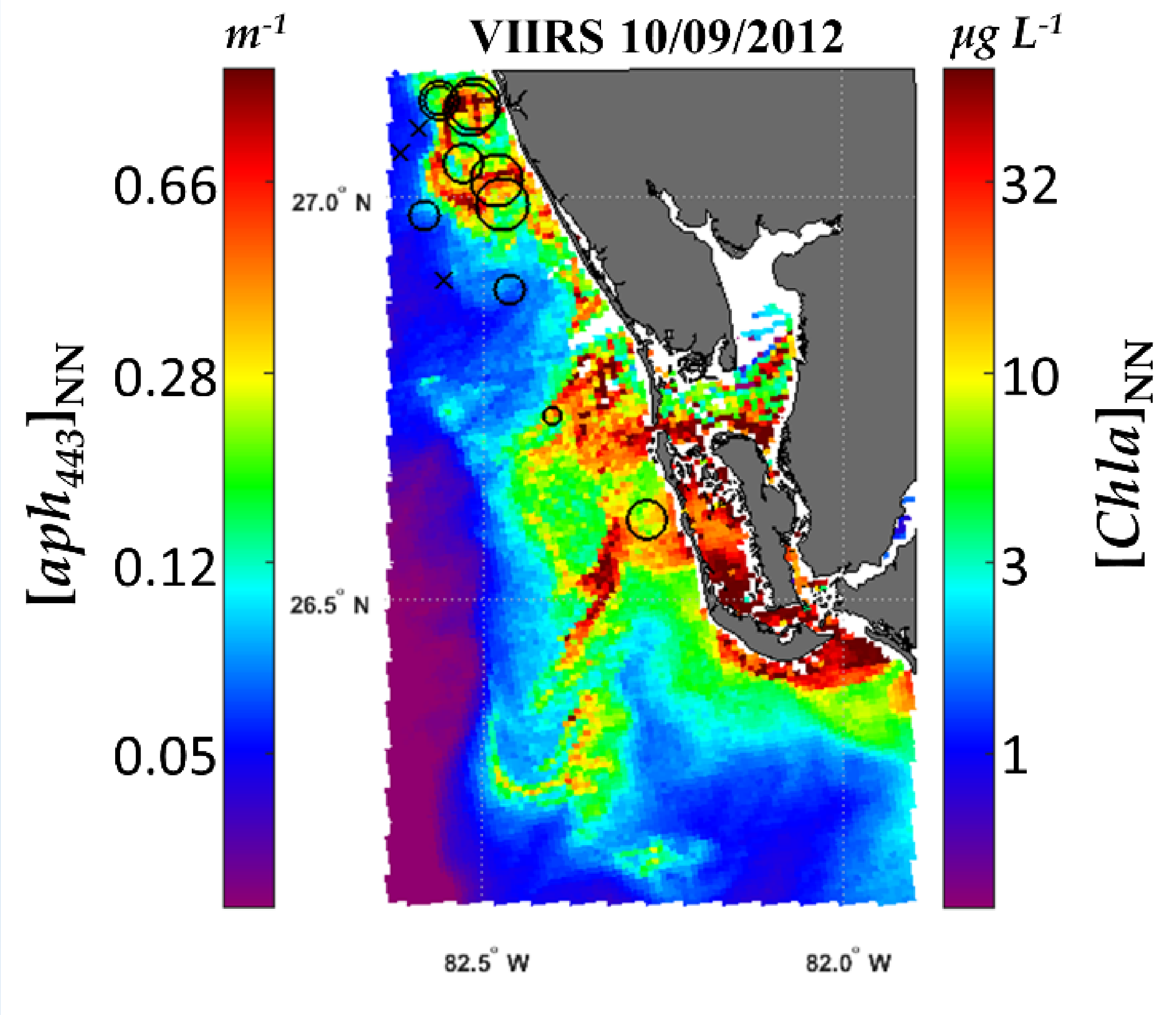

- Reflectance data obtained from the NASA Level 2, L2gen data processing system.

- Any individual pixel is excluded from the image if it has been flagged land, cloud, failure in atmospheric correction, bad navigation quality, both high and moderate glint, negative Rayleigh-corrected radiance

a_{ph443} : phytoplankton absorption at 443 nm.

[*Chla*] : Chlorophyll-a concentrations

Approach applied in WFS for *KB*-HABs Retrievals

- **First** we relate VIIRS Rrs (486,551,671) to $a_{ph}443$ using NN for estimation of $a_{ph}443$ which is approximately proportional to [*Chla*].

- **Then**, in a second critical step, we evolve limiting criteria which make use of two facts (*Cannizzaro, 2009*)

I. *low backscatter*	bb_p551	$\leq$ *max specific value.*		
&Equiv.	Rrs_{551}	$\leq$	$0.006\ sr^{-1}$	*Filter F1*
II. a_{ph443}		$\geq$ *min specific value.*		
	a_{ph443}	$\geq$	$0.061\ m^{-1}$	*Filter F2*

← *KB* blooms are ineffective backscatterer

These limiting criteria are applied to retrieved VIIRS retrievals of a_{ph443} & Rrs_{551} to effectively delineate and quantify *KB*.

Blooms on 10/09/2012

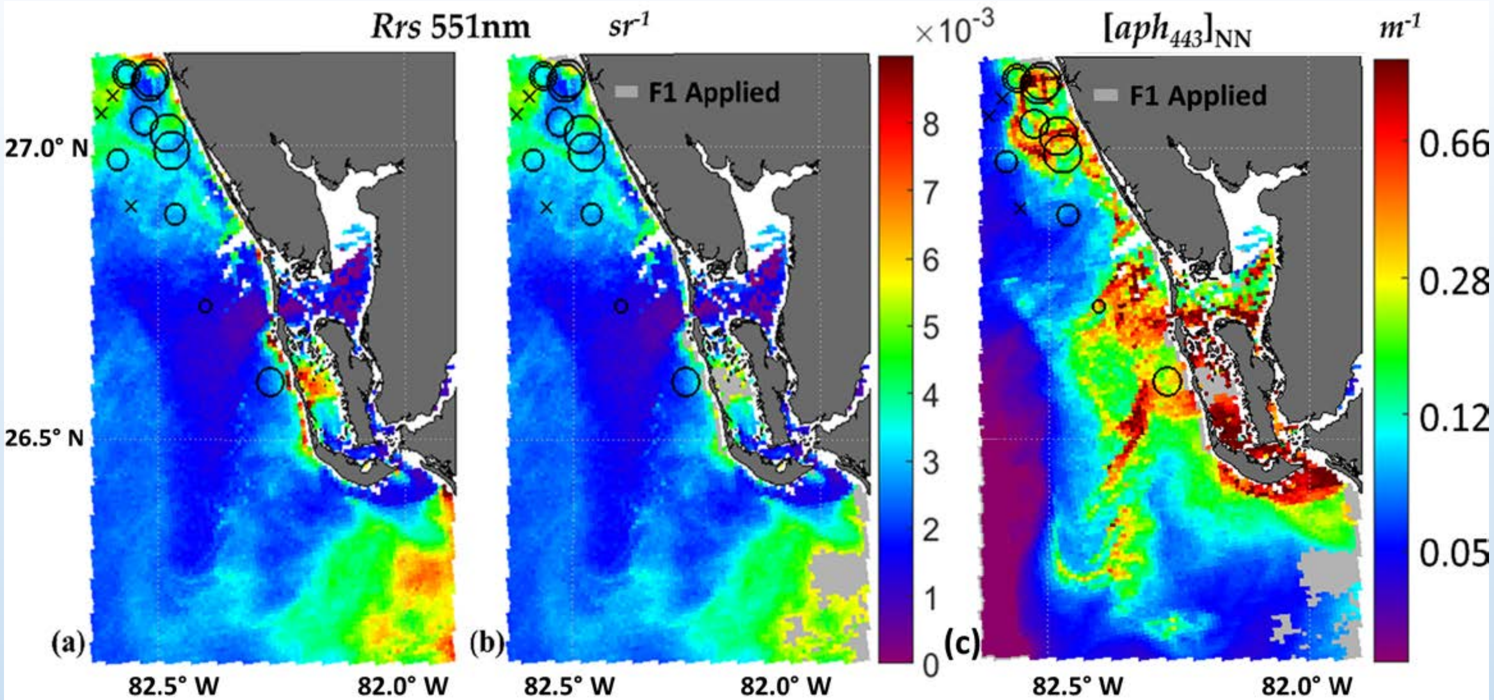

KB in-situ measurements:

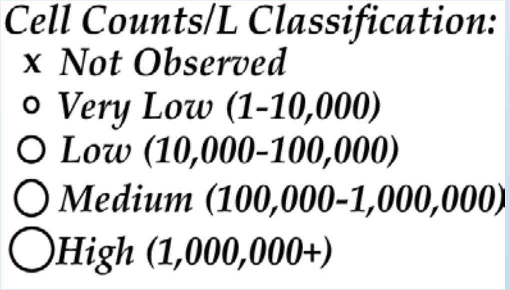

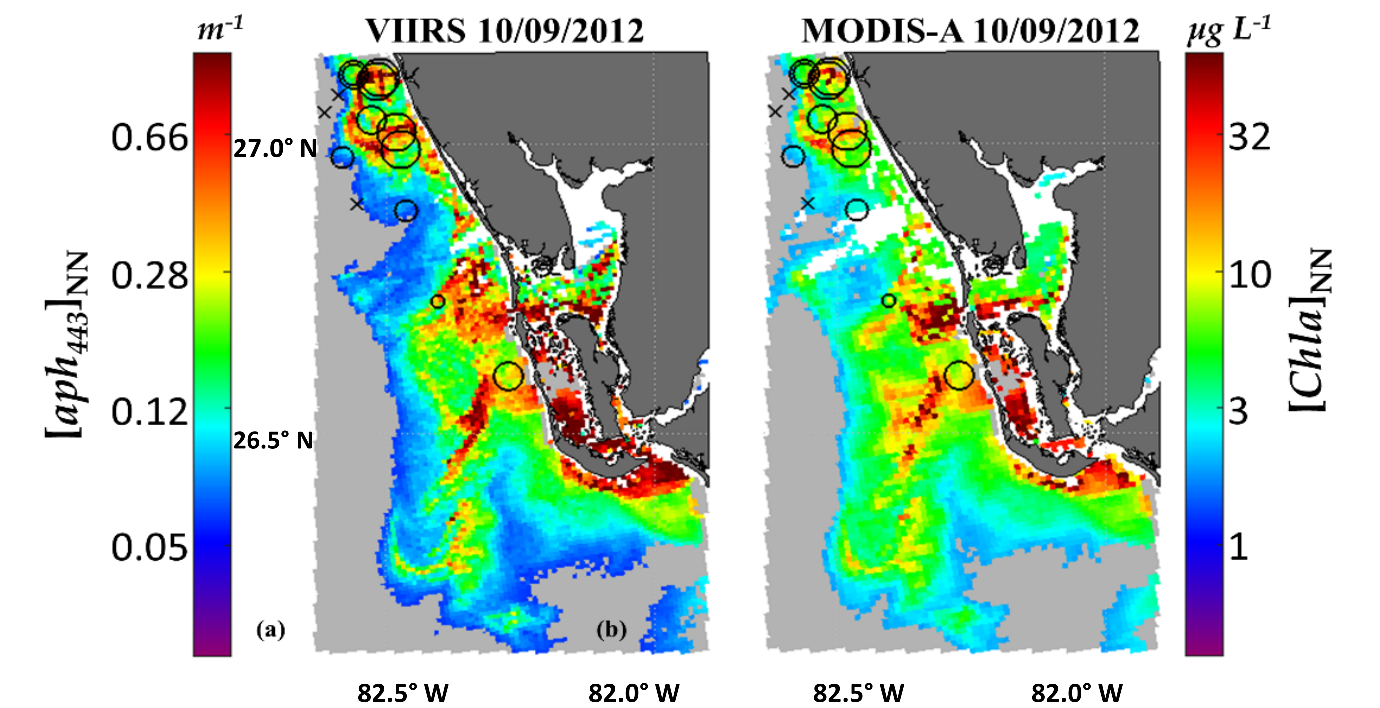

Successive applications of backscatter filter F1, and min a_{ph443} filter F2 (light grey) to NN VIIRS and MODIS retrievals so residual images show *KB* HABs

NN VIIRS retrievals compared against near-coincident in-situ *Karenia Brevis* (*KB*) cell counts (2012-2016)

- To obtain sufficient numbers of points for statistically meaningful comparisons all *Karenia Brevis* cell counts collected by Florida Fish and Wildlife Conservation Commission (FWC) over 2012-16 period were compared to all valid near coincident VIIRs retrievals. Comparisons of retrievals V in-situ shown in the coming slides for following algorithms:

  ***NN* (Neural Network)**

  ***(Ocx)* Ocean Color product for chlorophyll-a (NASA).**

  ***(GIOP)* Generalized Inherent Optical Property model**

  ***(QAA_5)* Quasi-Analytical Algorithm version 5**

  ***(RGCI)* Red Green chlorophyll-*a* Index [*Chla*] retrievals for WFS [*L. Qi, C. Hu 2015*];**

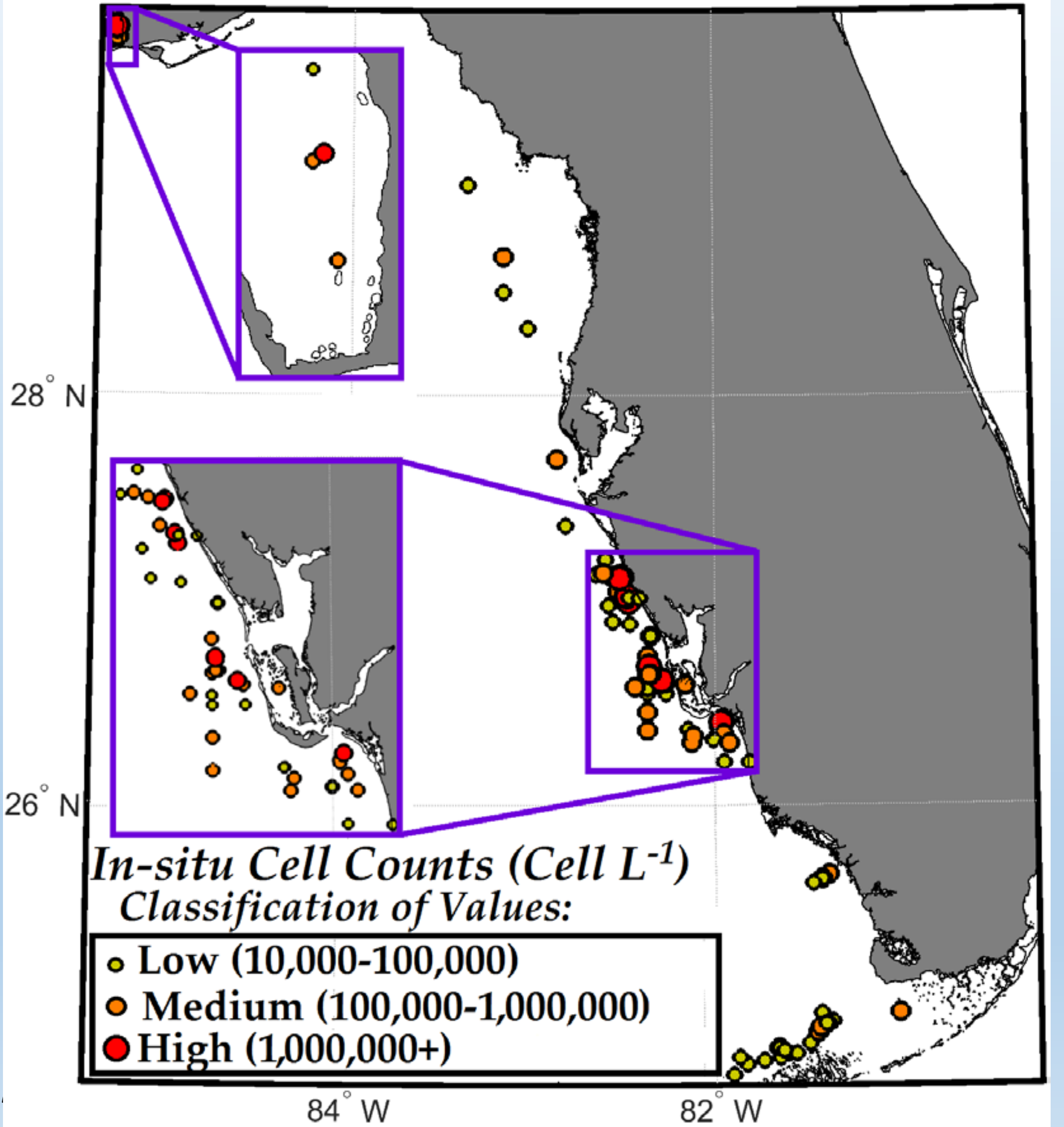

Retrieval comparisons using NN and other retrieval algorithms against in-situ cell counts

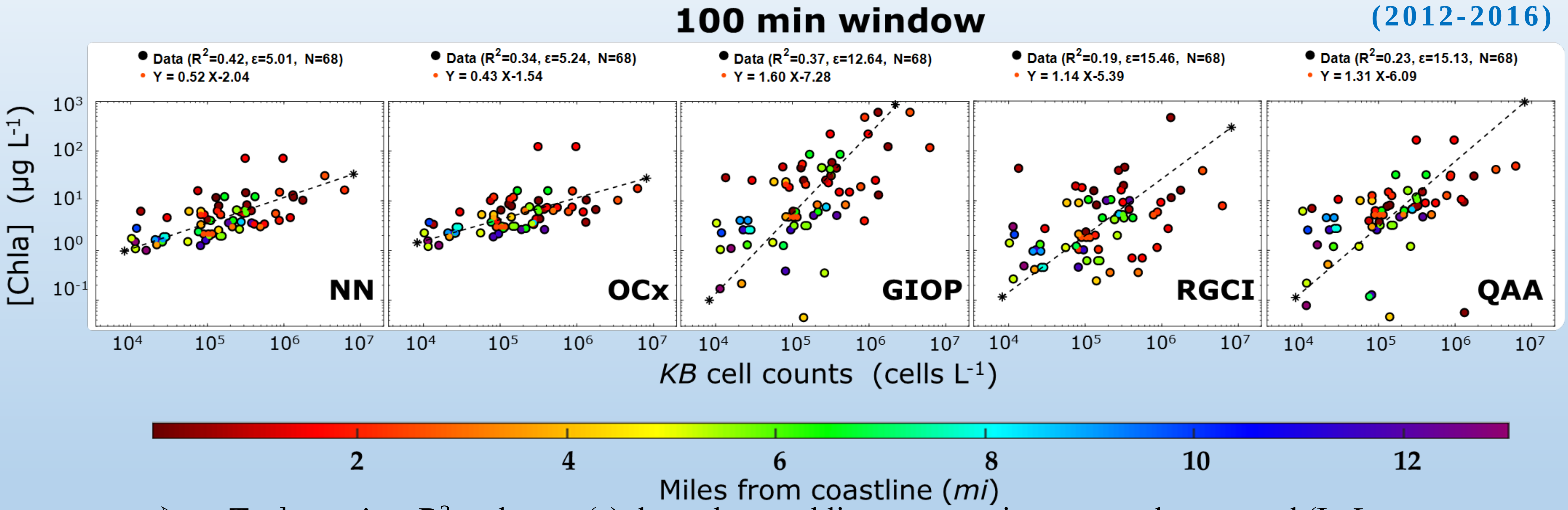

- ➢ To determine R^2 and error (ε) the orthogonal linear regression approach was used (L. Leng et al 2007).

Showing in-situ comparison for the 93 available match-ups points for 100 minutes overlap windows with in-situ observations obtained using the different algorithms (**NN, OCx, GIOP, RGCI**, and **QAA**$_{v5}$).

Data distribution comparison for *KB cell counts* in-situ measurements and equivalent their [Chla] retrieval algorithms

KB in-situ & retrievals algorithms		[*Chla*] data values ($\mu g \cdot L^{-1}$)						
		mean	**median**	**mode**	**STD**	**min**	**max**	**N**
In-situ	**VIIRS 100 minutes window**	4.1	1.4	0.8	9	0.1	62	68
NN		7.4	3.9	1.9	12	0.99	71	68
OCx		9	4.4	2.9	20	1.19	122	68
GIOP		50	10.6	3.1	118	0.04	597	68
RGCI		13.7	2.7	0.6	56	0.24	461	68
QAA_{v5}		13.7	6.2	3.2	28	0.05	163	68

To determine R^2 and error (ε) the orthogonal linear regression approach was used (L. Leng et al 2007), where errors are assumed to exist for both variables. The error (ε) is calculated as the sum of orthogonal distances. Results are shown in the next slide

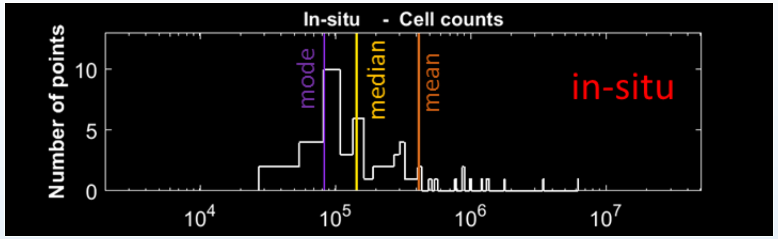

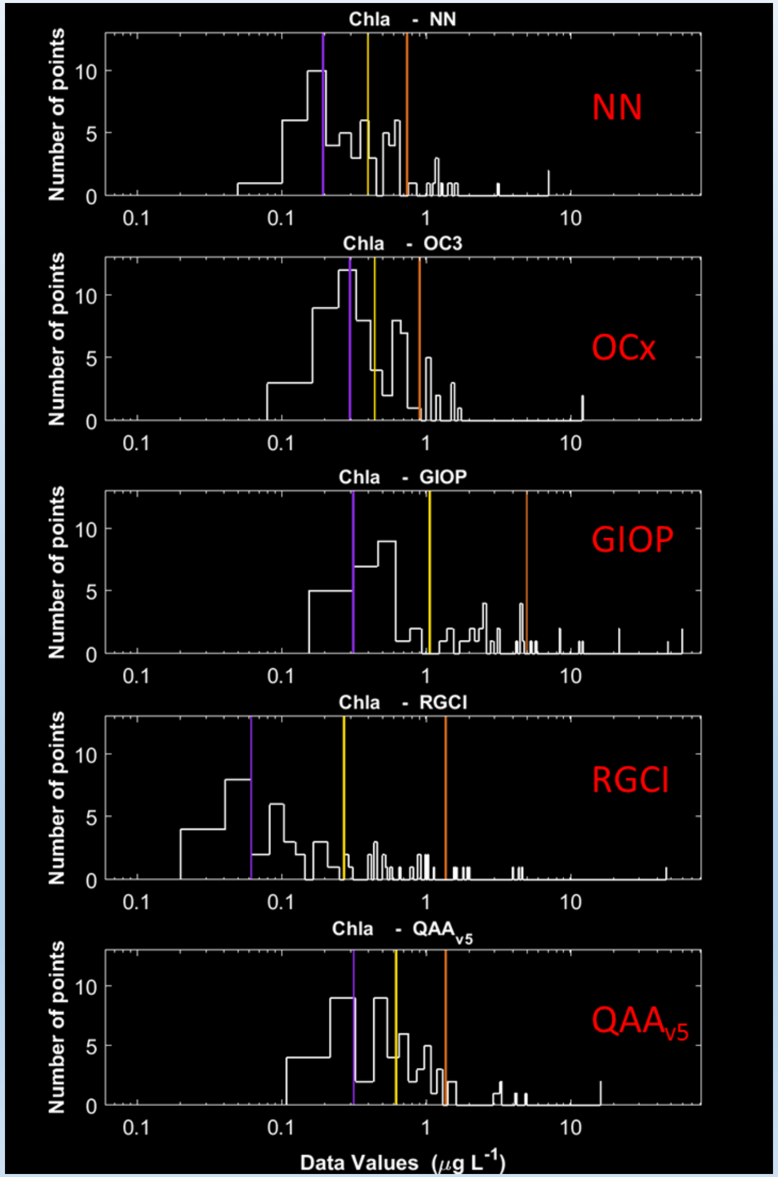

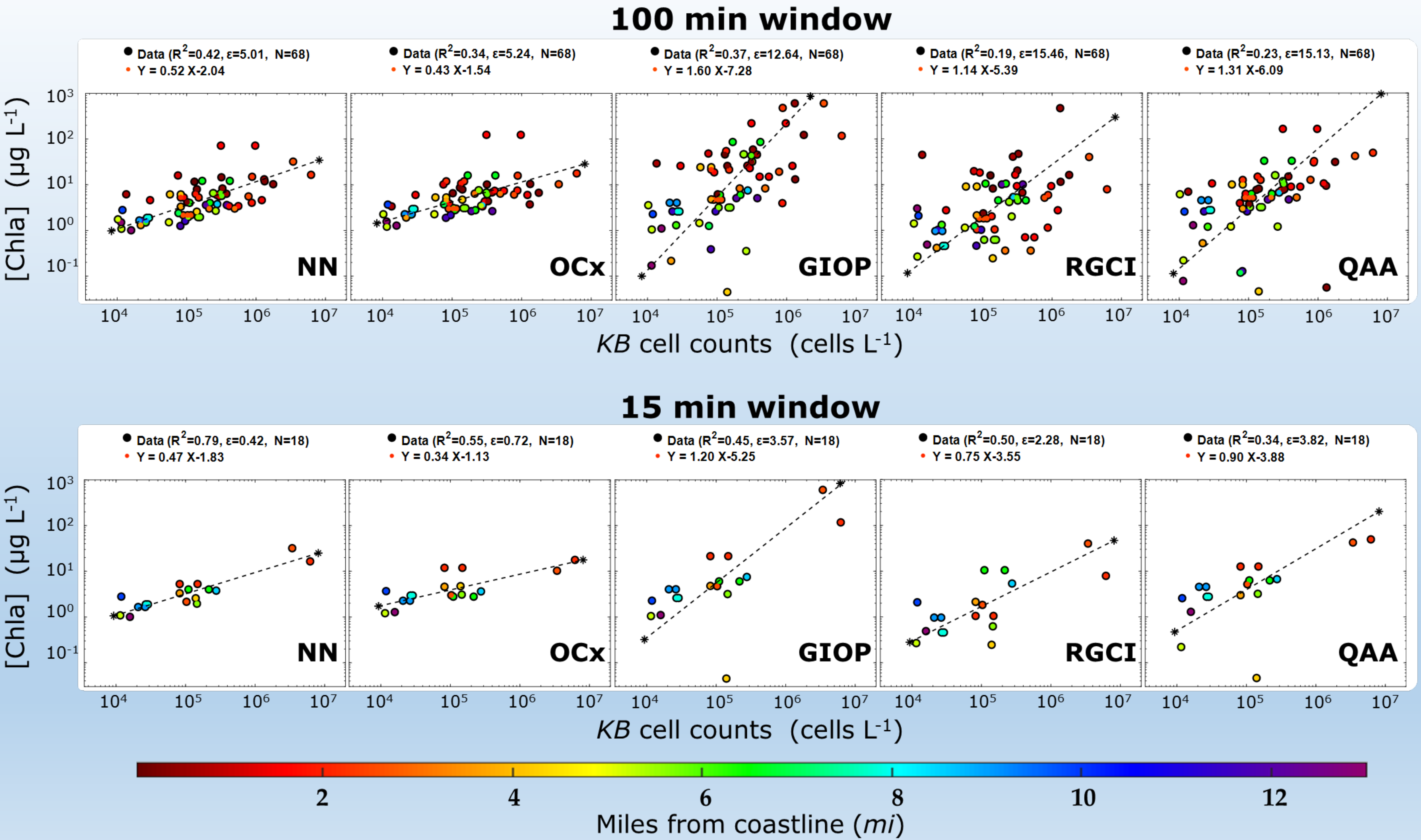

100 min window
Data (R2=0.42, ε=5.01, N=68)
Y = 0.52 X-2.04
Data (R2=0.34, ε=5.24, N=68)
Y = 0.43 X-1.54
Data (R2=0.37, ε=12.64, N=68)
Y = 1.60 X-7.28
Data (R2=0.19, ε=15.46, N=68)
Y = 1.14 X-5.39
Data (R2=0.23, ε=15.13, N=68)
Y = 1.31 X-6.09
NN
OCx
GIOP
RGCI
QAA
[Chla] (μg L-1)
KB cell counts (cells L-1)
15 min window
Data (R2=0.79, ε=0.42, N=18)
Y = 0.47 X-1.83
Data (R2=0.55, ε=0.72, N=18)
Y = 0.34 X-1.13
Data (R2=0.45, ε=3.57, N=18)
Y = 1.20 X-5.25
Data (R2=0.50, ε=2.28, N=18)
Y = 0.75 X-3.55
Data (R2=0.34, ε=3.82, N=18)
Y = 0.90 X-3.88
NN
OCx
GIOP
RGCI
QAA
[Chla] (μg L-1)
KB cell counts (cells L-1)
2
4
6
8
10
12
Miles from coastline (mi)

Summary table

y-axis [*Chla*] ($\mu g \cdot L^{-1}$)	*x-axis* *KB* Cell Counts (*cells* L^{-1})	R^2	ε	Slope & Intercept	N
NN	**VIIRS 100 minutes window**	0.42	5.01	$y = 0.52\,x - 2.04$	68
OCx		0.34	5.24	$y = 0.43\,x - 1.54$	68
GIOP		0.37	12.64	$y = 1.60\,x - 7.28$	68
RGCI		0.19	15.46	$y = 1.14\,x - 5.39$	68
QAA		0.23	15.13	$y = 1.31\,x - 6.09$	68
NN	**VIIRS 15 minutes window**	0.79	0.42	$y = 0.47\,x - 1.83$	18
OCx		0.55	0.72	$y = 0.34\,x - 1.13$	18
GIOP		0.45	3.57	$y = 1.20\,x - 5.25$	18
RGCI		0.50	2.28	$y = 0.75\,x - 3.55$	18
QAA		0.34	3.82	$y = 0.90\,x - 3.88$	18

Table: Statistics of comparison for retrieval algorithms and there successful retrievals against in-situ observations (2012-2016)

Consecutive satellite images on Nov. 3rd 2014

Showing variation in bloom.

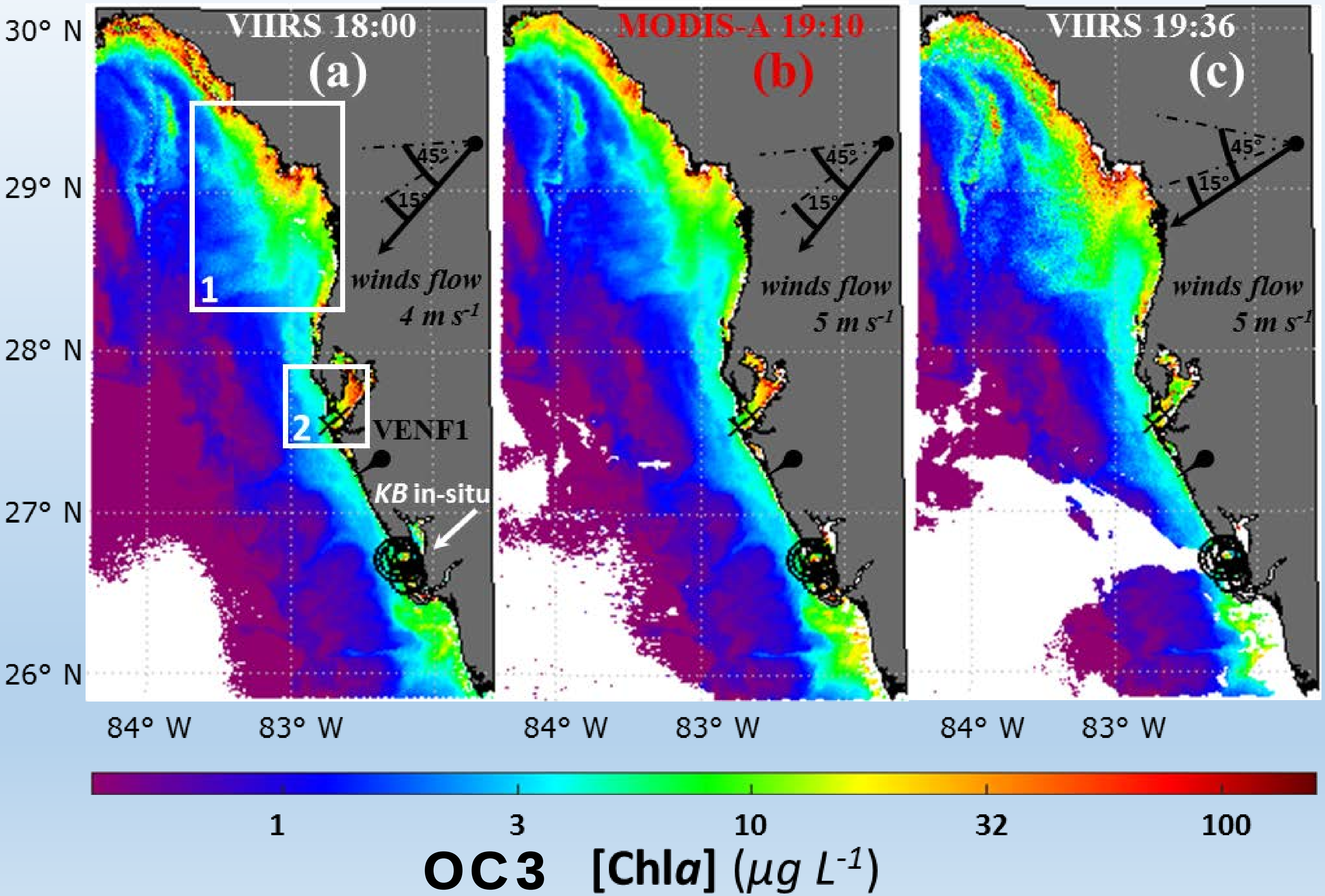

Changes in bloom for consecutive satellite images of region 1 using retrieved OC3 [*Chla*].

- The bloom, as delineated by the [*Chla*] color contour in the images, appears, qualitatively, to increase in concentration and expand in the southwest direction over the 96 minute interval between the consecutive overlapping VIIRS-MODIS-VIIRS images.

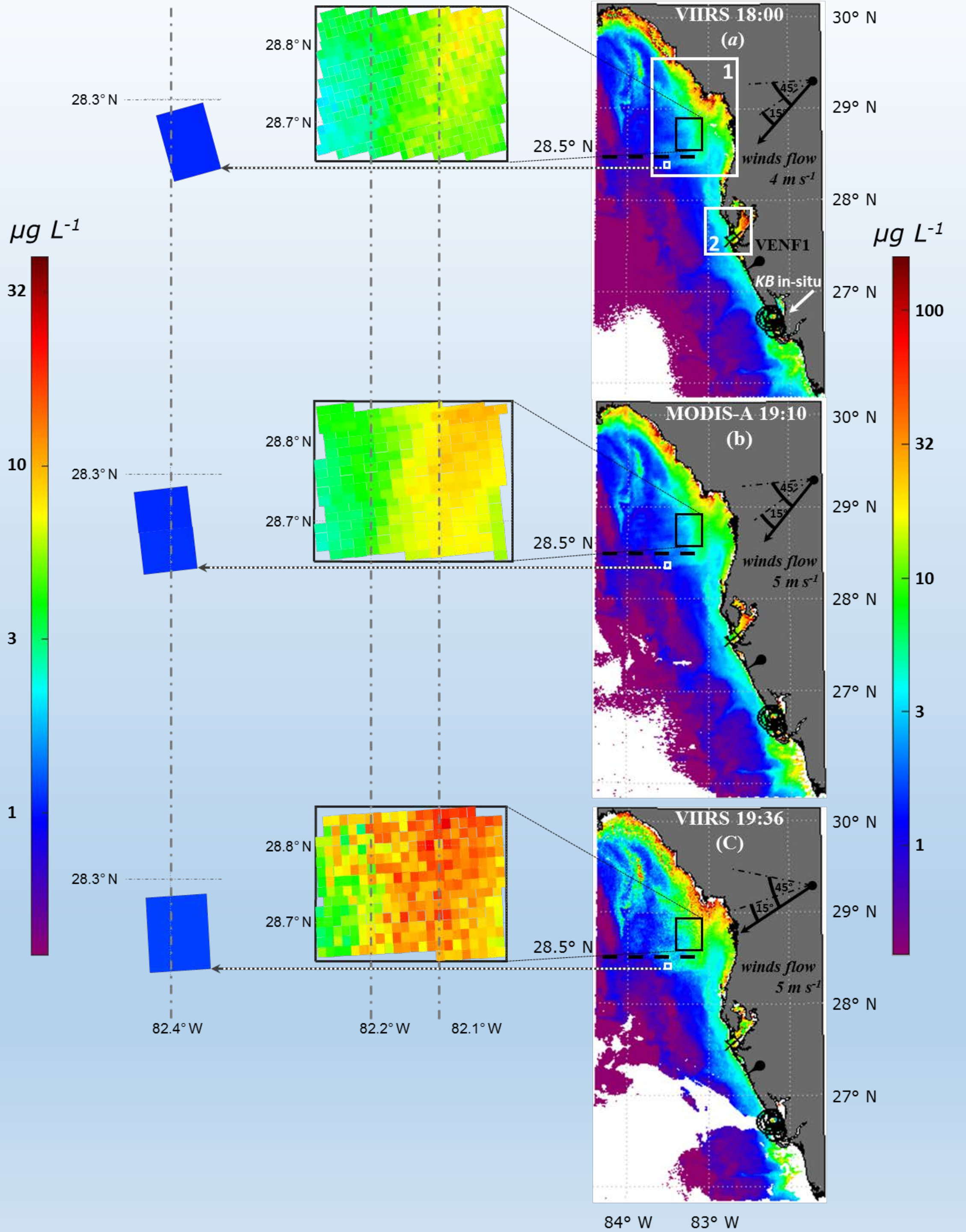

region 1 using NN retrieved [*Chla*].

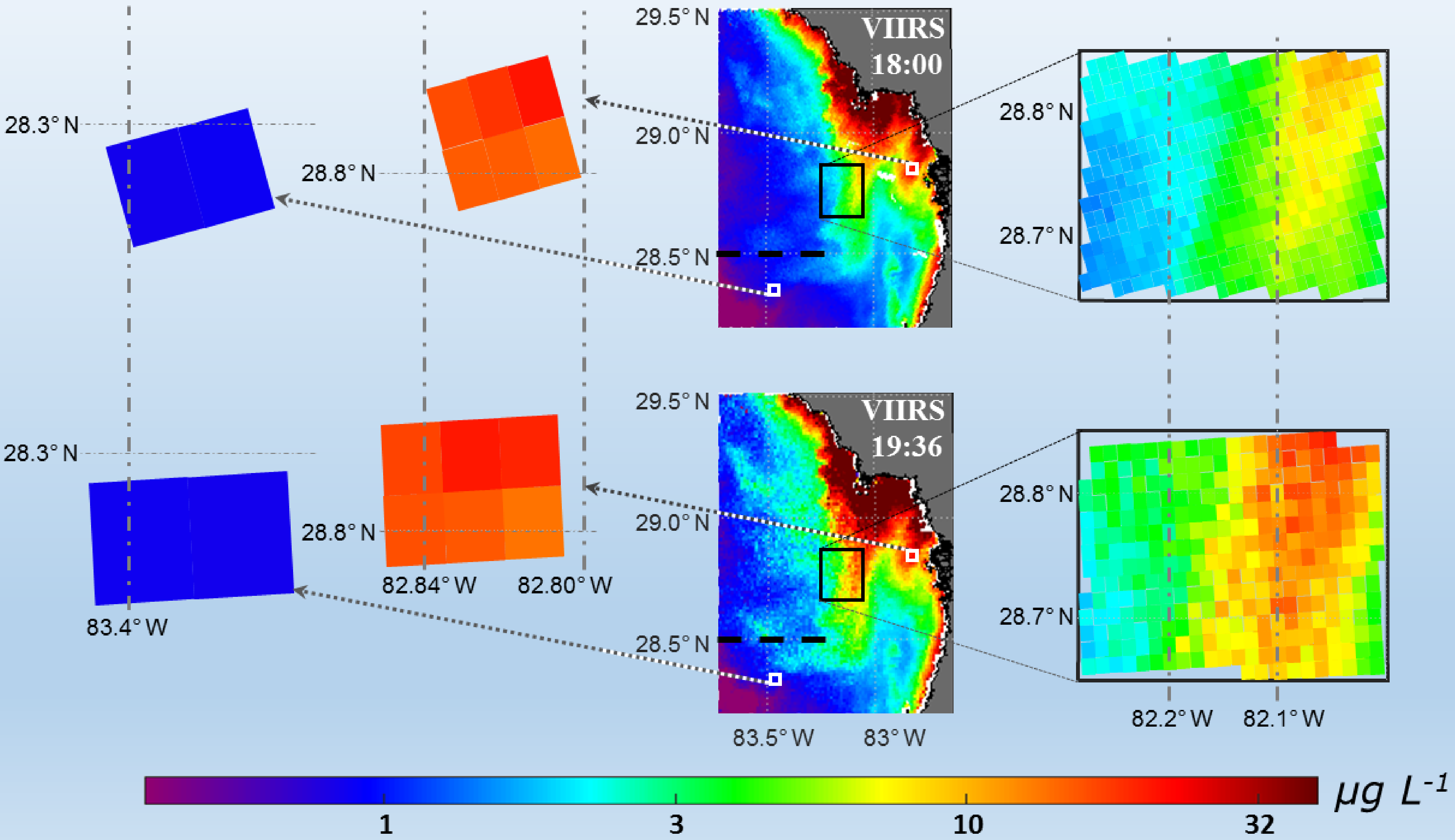

NN retrievals from Tampa Bay, Region 2.

Figure shows VIIRS and MODIS-A sequential retrievals from Tampa Bay, where a bloom seems to shrink in [*Chla*] densities opposite to the wind and current direction, implying that there are a complexity of factors at work, possibly including downwelling.

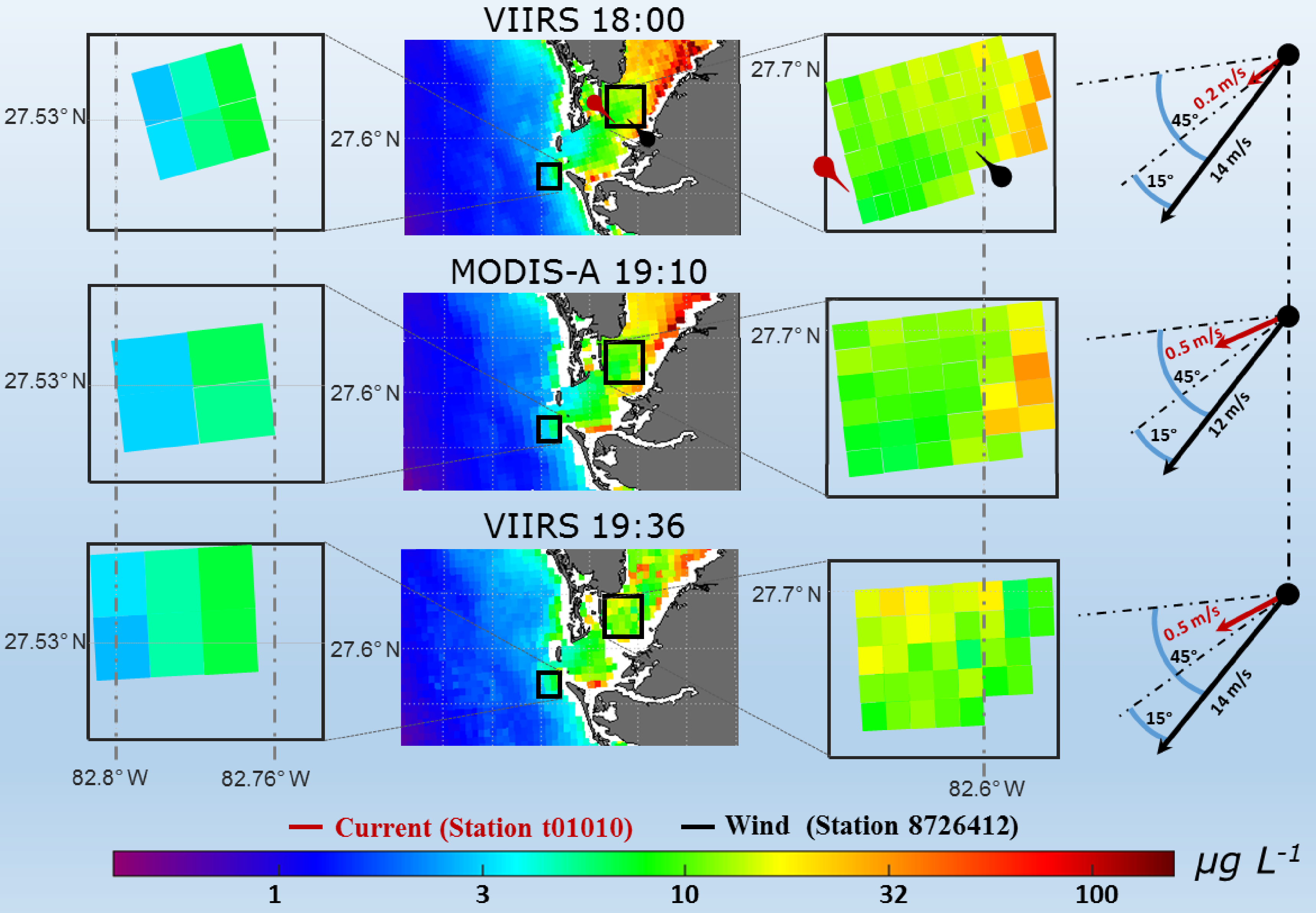

Results of field measurements showing temporal variability on 1/19/2017

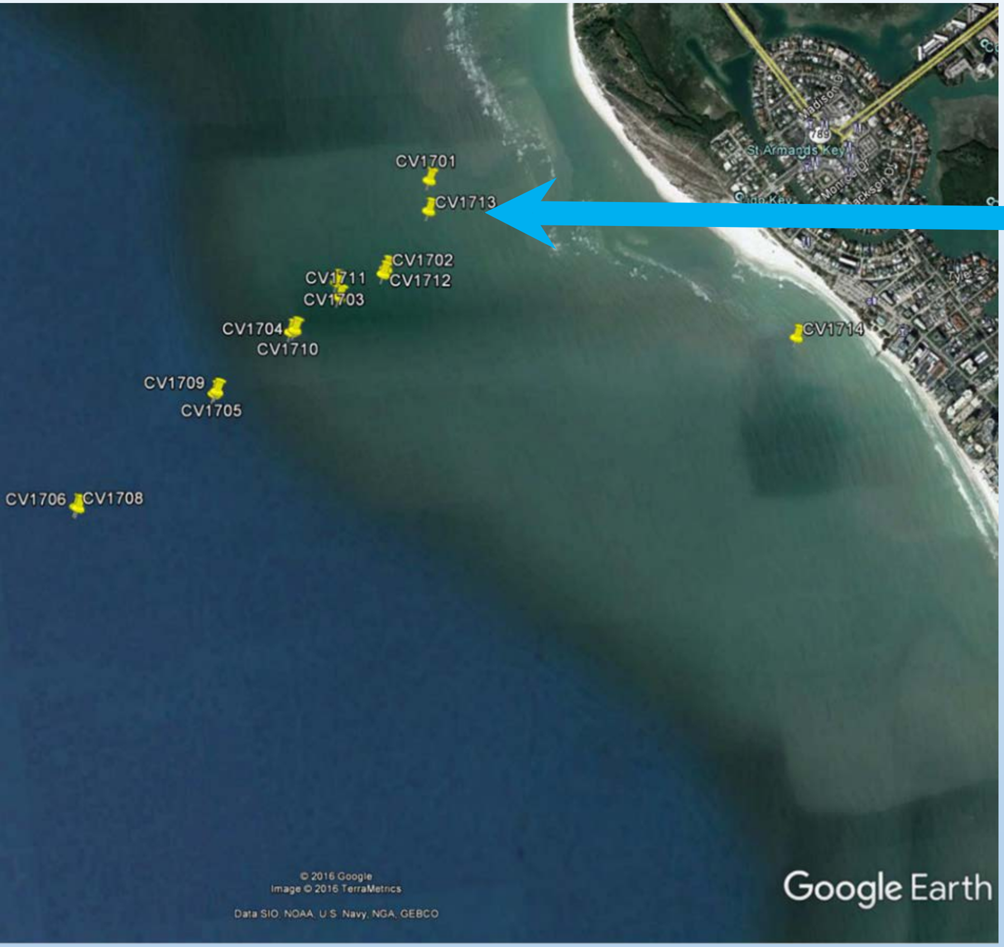

Figure Transect of outward and return legs of field measurements.

Station	Depth (m^{-1})	Lat. (°)	Long. (°)	Start Time (*GMT*)	End Time (*GMT*)	*K. brevis* (*cells L^{-1}*)	Time diff (*minutes*)
CV1701	0.7	27.31836	-82.59587	17:20	17:25	**7,280,000**	**120**
CV1713	0.7	27.31713	-82.59606	19:21	19:25	**1,552,000**	
CV1702	0.7	27.31500	-82.59831	17:48	17:52	**1,776,000**	**87**
CV1712	0.7	27.31480	-82.59846	19:15	19:19	**1,326,000**	
CV1703	0.7	27.31467	-82.60061	18:00	18:04	**1,024,000**	**68**
CV1711	0.7	27.31408	-82.60059	19:09	19:12	**1,110,000**	
CV1704	0.7	27.31296	-82.60277	18:07	18:12	**964,000**	**54**
CV1710	0.7	27.31289	-82.60298	19:03	19:06	**590,000**	
CV1705	0.7	27.31077	-82.60677	18:18	18:22	**642,000**	**37**
CV1709	0.7	27.31085	-82.60664	18:55	18:59	**576,000**	
CV1706	0.7	27.30681	-82.61356	18:27	18:32	**952,000**	**21**
CV1708	0.7	27.30686	-82.61364	18:48	18:51	**690,000**	

These results illustrate both the intra pixel variations that can typically occur (as well as inter pixel variations) and also confirm the temporal variations that can be expected. The relative contributions of drift or upwelling/downwelling to the results are not known.

Conclusion

- The use of NN retrievals of $a_{ph}443$ from VIIRS show promise as a viable algorithm for the Florida coastal regions with complex water conditions.
- Comparisons against in-situ measurements show that VIIRS [Chl$a$] data retrievals are significantly improved for all algorithms for shorter overlap time windows.
- Show important impact of temporal variations on retrieval accuracies.
- Further detailed comparisons with in-shore in-situ measurements are planned and considerations of subpixel variability addressed.

Acknowledgment

We thank NOAA JPSS and NOAA-Crest for the support to continue this work.

Thank you